Available online at www.sciencedirect.com
ScienceDirect
Journal of Molecular Spectroscopy 242 (2007) 1–9
Journal of MOLECULAR SPECTROSCOPY
www.elsevier.com/locate/jms

Intracavity laser absorption spectroscopy of D_2O between 11 400 and 11 900 cm^{-1}

O.V. Naumenko [a], F. Mazzotti [b], O.M. Leshchishina [a], J. Tennyson [c], A. Campargue [b,*]

[a] Institute of Atmospheric Optics, Russian Academy of Sciences, Tomsk, 634055, Russia
[b] Laboratoire de Spectrométrie Physique (associated with CNRS, UMR 5588), Université Joseph Fourier de Grenoble, B.P. 87, 38402 Saint-Martin-d'Hères, Cedex, France
[c] Department of Physics and Astronomy, University College London, London WC1E 6BT, UK

Received 11 December 2006; in revised form 5 January 2007
Available online 12 January 2007

Abstract

The weak absorption spectrum of dideuterated water, D_2O, has been recorded by Intracavity Laser Absorption Spectroscopy (ICLAS) between 11 400 and 11 900 cm^{-1}. This spectrum is dominated by the $3\nu_1 + \nu_2 + \nu_3$ and the $\nu_1 + \nu_2 + 3\nu_3$ centered at 11 500.25 and 11 816.64 cm^{-1}, respectively. A total of 530 energy levels belonging to eight vibrational states were determined. The rovibrational assignment process of the 840 lines attributed to D_2O was mostly based on the results of new variational calculations consisting in a refinement of the potential energy surface of Shirin et al. [J. Chem. Phys., 120 (2004) 206] on the basis of recent experimental observations, and a dipole moment surface from Schwenke and Partridge [J. Chem. Phys. 113 (2000) 6592]. The overall agreement between these calculations and the observed spectrum is very good both for the line positions and the line intensities.

Keywords: Water; D_2O; Intracavity laser absorption spectroscopy; ICLAS; Rovibrational assignment; Deuterated water

1. Introduction

The experimental absorption spectrum of D_2O in the near IR region is less well characterized than that of the monodeuterated species, HDO. The previous analyses of the D_2O absorption features above 10 000 cm^{-1} are limited to two recent studies: the most intense $3\nu_1 + \nu_3$ band was investigated between 10 200 and 10 440 cm^{-1} by Fourier transform spectroscopy (FTS) with a 105 m path length [1], while the absorption in the 12 570–12 820 cm^{-1} spectral region, mostly due to the $4\nu_1 + \nu_3$ band, was recorded by Intracavity Laser Absorption Spectroscopy (ICLAS) with a FTS detection scheme [2].

The present contribution is devoted to the 11 400–11 900 cm^{-1} region, where the D_2O spectrum is dominated by two well separated bands (see Fig. 1): the $3\nu_1 + \nu_2 + \nu_3$ and the $\nu_1 + \nu_2 + 3\nu_3$ centered at 11 500.247 and 11 816.636 cm^{-1}, respectively, belonging to the $(\nu_1 + \nu_2/2 + \nu_3) = 4.5$ polyad which is the first pentadecad of resonating states. We have recently reported the analysis of the second decad lying in the 8800–9520 cm^{-1} from a combined study by FTS with a 600 m path length in Reims and by ICLAS based on vertical external cavity surface emitting lasers (VeCSEL) in Grenoble [3]. This work showed that, in this spectral range, the two experimental approaches have specific advantages but a roughly equivalent sensitivity. To the best of our knowledge, the only available spectrum of D_2O in the region under consideration is that recorded with the same FTS spectrometer by the Reims–Brussels collaboration. The analysis of this FTS spectrum in a wider region will be published separately [4] but only 71 D_2O lines, all lying below 11 581 cm^{-1}, are observed by FTS between 11 400 and 11 900 cm^{-1} while we could identify more than 1200 lines by ICLAS. Indeed, the ICLAS detection limit achieved in the 10 000–14 000 cm^{-1} with a Titanium Sapphire laser is significantly better than that provided by ICLAS-VeCSEL below 10 000 cm^{-1}.

* Corresponding author. Fax: +33 4 76 63 54 95.
E-mail address: Alain.Campargue@ujf-grenoble.fr (A. Campargue).

0022-2852/$ - see front matter © 2007 Published by Elsevier Inc.
doi:10.1016/j.jms.2007.01.001

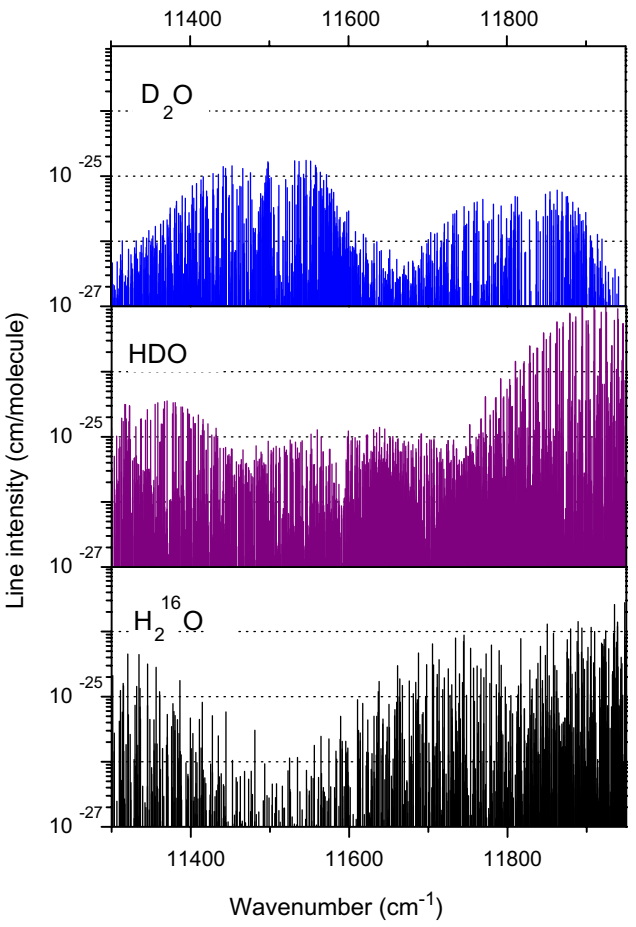

Fig. 1. Overview of the D_2O, HDO and H_2O spectra between 11 300 and 11 950 cm^{-1} as calculated by Schwenke and Partridge [11,13]. Note the logarithmic scale adopted for the line intensity values. The line intensities correspond to the pure species.

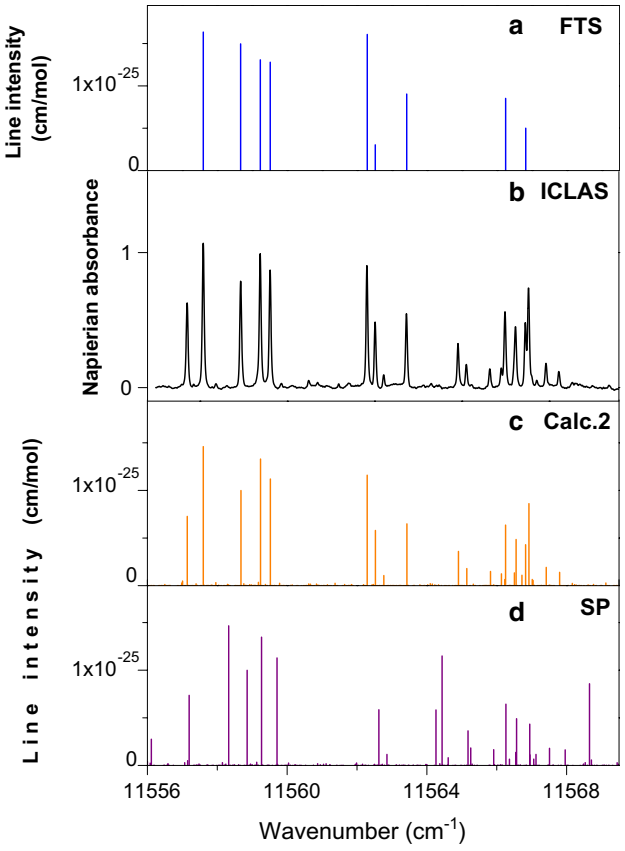

Fig. 2. Comparison of the D_2O spectrum around 11 560 cm^{-1}: (a) FTS spectrum [4], (b) ICLAS spectrum ($P \approx 20$ hPa, $l_{eq} \approx 14.4$ km) (c) results of the new variational calculations of Ref. [18] and (d) results of the calculations of Schwenke and Partridge [11,13].

An overview of the D_2O, HDO, and H_2O stick spectra in the region of interest is presented in Fig. 1. The global comparison of the line intensities (for the pure species) shows that up to about 11 800 cm^{-1}, the HDO and D_2O line intensities are on the same order of magnitude while the $H_2{}^{16}O$ absorption is weaker in the 11 400–11 600 cm^{-1} region. In fact, no $H_2{}^{16}O$ lines were detected in our spectra as the numerous successive fillings and emptyings of the intracavity cell (see below) almost completely washed out the $H_2{}^{16}O$ adsorbed on the walls of the cell.

2. Experimental details

Our ICLAS experimental apparatus has been previously described [6,7]. The spectra were recorded with a generation time of 150 μs corresponding to an equivalent absorption path length of 14.4 km, as the filling ratio of the laser cavity by the absorption cell was 32%. The intracavity sample cell was filled with D_2O (Aldrich, 99.96% D) at pressures up to 20 hPa. In order to minimize the contribution of the intracavity atmospheric absorption, the laser was placed in a box filled with dry nitrogen. The experimental procedure consisted in successively filling the cell with water, recording the spectrum, evacuating the cell and recording the background spectrum. This procedure has both the advantage of increasing the signal to noise ratio (see Refs. [8,9]) and washing out natural water from the cell. Indeed, due to the rapid proton exchange between D_2O introduced in the gas phase and H_2O adsorbed on the wall of the cell, D_2O replaces H_2O progressively, leading to a very high deuterium enrichment. From the absorbance of HDO transitions detected at high energy, we estimated the relative concentration of HDO and D_2O to be 2% and 98%, respectively, $H_2{}^{16}O$ concentration being negligible. With such deuterium enrichment, the D_2O transitions could be observed above 11 800 cm^{-1}, while they are typically two orders of magnitude weaker than HDO transitions in that region. Two examples of spectra are displayed in Figs. 2 and 3.

The ICLAS spectrum is recorded in successive 12 cm^{-1} wide spectral sections. The wavenumber calibration of each individual spectrum requires the use of reference lines. They were taken from Ref. [4] below 11 600 cm^{-1} while above 11 750 cm^{-1} we used HDO lines from Ref. [10]. We had difficulties in the intermediate region so additional spectra with a higher HDO concentration were recorded in order to provide reference lines.

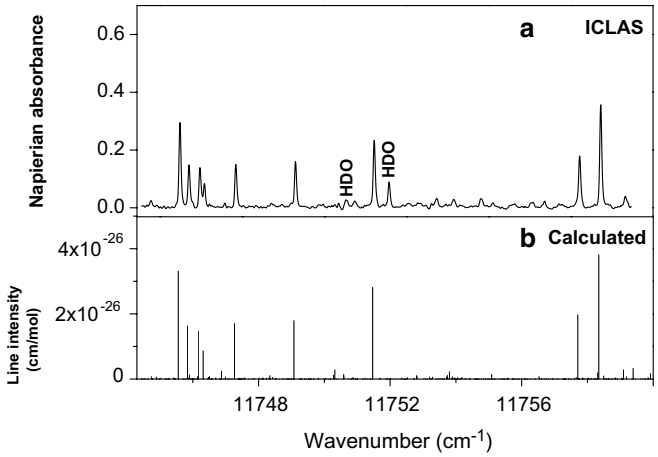

Fig. 3. Comparison of the D_2O spectrum around 11 750 cm^{-1}: (a) ICLAS spectrum ($P \approx 20$ hPa, $l_{eq} \approx 14.4$ km) and (b) results of the new variational calculations of Ref. [18]. In this spectral section, no lines were detected in the FTS spectrum of Ref. [4].

For each individual spectrum, a line list was created containing the line centers and the corresponding relative intensities obtained by fitting the line contour as a single Gaussian profile with homemade software which saved the line center as well as the line area. Obviously, in the case of overlapping lines, this rough procedure led to an underestimation of the intensities. We then applied a multi-Gaussian fit procedure in the specific spectral sections showing blended lines in order to retrieve more accurate relative line intensities. The retrieved relative line intensities in each elementary spectrum were then scaled against the values predicted by the new variational calculations presented below (''calculations 2''). The most complete list was created simply by gathering all the line lists corresponding to the individual spectral windows. In this global list, many lines appear several times as a consequence of several recordings of the same spectral windows and of the existence of overlapping regions. As the accuracy of the ICLAS line positions was estimated to be around 0.004 cm^{-1}, we decided to consider two lines as identical when both their wavenumber difference was less than 0.008 cm^{-1} and their intensity differed by at most a factor of 2. This global line list was then further checked and cleaned of spurious lines or irreproducible spectral features close to the noise level. HDO lines were also identified from our recent ICLAS study [5] leading to a list of 840 D_2O transitions which is the one considered in the following rovibrational analysis.

3. Spectrum assignment and results

Since the achievements in the theoretical modelling of the rovibrational molecular spectra [11,12] in 1997, the assignment of the high resolution water vapor and its isotope substituted species spectra is generally performed on the basis of high accuracy variational linelists. As no optimization of the Partridge and Schwenke potential energy surface (PES) [11] was performed to the experimental data in the case of the D_2O isotopologue, the results of their calculations [11,13] are not fully satisfactory (see lower panel of Fig. 2). As the first stage in our analysis, we then used the improved identification list based on the PES of Ref. [14] and the dipole moment surface (DMS) of Ref. [13], which we refer below as ''calculation 1''. Rovibrational labels were transferred from Ref. [15] dataset obtained using the Partridge and Schwenke PES and DMS [11,13]. Most of the strong lines, which belong, mainly, to the (3 1 1)–(0 0 0) and (1 1 3)–(0 0 0) bands with low J and K_a values were confidently assigned in this way. However, we experienced difficulties in assigning the transitions belonging to much weaker bands or those of the strong bands with high J and K_a values, since some of the observed positions were found to deviate greatly (up to 1.2 cm^{-1}) from their predicted values. These weak transitions, as a rule, are not involved in combination differences (CD) in the ground state, and their identification relies almost entirely on the good correspondence between theory and experiment.

It was clear that new calculations were required since the available experimental D_2O energy levels set used to optimize the previous D_2O PES [14] was too limited, leading to important deviations from the current observations. Thus, the new experimental energy levels obtained at the

Table 1
Summary of the spectroscopic information obtained by ICLAS for D_2O in the 11 400–11 906 cm^{-1} region

Vibrational state	Band origin (cm^{-1})		Intensity (cm/molecules)		I_{obs}/I_{calc}	N Lines	N Levels
	Obs.	Calc.[a]	Obs.	Calc.[a]			
330		11245.68	1.736E − 26	1.616E − 26	1.07	5	5
231		11289.72	9.40E − 26	9.40E − 26	1.00	13	9
132		11441.21	1.116E − 25	1.136E − 25	0.98	21	18
410	11483.6393	11483.65	6.52E − 25	7.32E − 25	0.89	110	85
311	11500.2475	11500.25	9.04E − 24	9. 40E − 24	0.96	317	160
033	11605.79[b]	11605.75	1.42E − 25	1.172E − 25	1.21	68	45
212	11679.3894	11679.27	4.00E − 25	4.24E − 25	0.94	166	94
113	11816.6366	11816.58	2.892E − 24	2.876E − 24	1.01	256	114

[a] Calculated values from Ref. [18].
[b] Estimated value see text.

Table 2
Rovibrational term values (cm^{-1}) of the (311), (113), (212) and (410) vibrational states of D_2O

J	K_a	K_c	(311)			(113)			(212)			(410)		
			E_{obs}	σ	N	E_{obs}	σ	N	E_{obs}	σ	N	E_{obs}	σ	N
0	0	0	11500.2475		1	11816.6366		1	11679.3894		1	11483.6393		1
1	0	1	11511.9563	0.6	2	11828.3730	0.4	2				11495.2520		1
1	1	1	11520.0329	0.1	2	11835.9523	2.5	2	11699.1748	1.8	2	11503.5772	2.9	2
1	1	0	11522.5843	1.8	2	11838.5539	7.6	2	11701.7122		1	11506.1443		1
2	0	2	11534.7772	0.6	2	11851.2871	2.9	2	11713.7678	0.4	2	11517.9889	1.6	2
2	1	2	11540.5898	1.0	3	11856.8406	1.4	3				11524.1864		1
2	1	1	11548.0983	1.5	3	11864.6464	1.7	3	11727.5167	2.1	2	11531.8869	0.4	2
2	2	1	11572.7672	0.5	2	11887.2864	3.3	2	11751.8764	2.4	2	11557.3451		1
2	2	0	11573.2801	1.1	2	11887.8513	3.9	2	11752.3728	0.2	2	11557.6904	3.5	2
3	0	3	11567.7719	1.7	2	11884.3863	1.4	2	11746.7405		1	11550.9477		1
3	1	3	11571.2743	1.9	3	11887.8341	0.0	2	11750.6805	1.4	2	11554.8897		1
3	1	2	11585.7610	0.4	3	11903.3445	2.4	2	11765.8571		1	11570.1362		1
3	2	2	11607.3799	1.1	3	11922.5529	2.4	2	11786.7830	5.5	2	11592.7993	0.8	2
3	2	1	11609.7989	0.5	3	11925.2030	1.2	2	11789.1638		1			
3	3	1	11654.6761	0.1	2	11966.7709	2.7	2	11833.6626		1			
3	3	0	11654.7426	1.7	2	11966.8493	1.7	2	11833.7083		1			
4	0	4	11610.0596	0.0	2	11926.7914	3.0	2	11789.0506		1	11593.2584		1
4	1	4	11611.8173	1.5	3	11928.6342	4.0	2	11791.2560		1	11595.4035		1
4	1	3	11634.4488	0.9	2	11954.0608	0.1	2	11816.1549	5.0	2	11620.3680	0.6	2
4	2	3	11653.1548	0.9	3	11969.0986	1.6	2	11832.9088	2.3	2	11640.3955	1.0	2
4	2	2	11659.6801	0.6	3	11976.2085	1.6	3	11839.4224		1	11644.4330		1
4	3	2	11701.7065	1.4	3	12014.8347	1.9	3	11881.0151		1	11688.2685		1
4	3	1	11702.1550	0.0	2	12015.3635	1.9	3	11881.4500	1.6	3	11688.5832		1
4	4	1	11766.1629		1	12074.7530	4.5	2	11944.8228		1	11756.3923		1
4	4	0	11766.1718		1	12074.7518		1	11944.8657	1.1	2	11756.3912		1
5	0	5	11661.2696	0.2	2	11978.1300	0.6	2	11840.2579		1	11644.4264		1
5	1	5	11662.0059	1.0	3	11978.9903	0.5	3	11841.2959		1	11645.4657		1
5	1	4	11700.3141	1.7	4	12015.9184	1.5	4	11877.6283	0.2	2	11681.8311	1.7	2
5	2	4	11709.8343	1.6	3	12026.5339	0.9	2	11890.4025 *	3.9	2	11692.8199		1
5	2	3	11722.8480	0.6	3	12040.7704	1.8	3	11903.1425	6.0	2	11707.8852		1
5	3	3	11760.5186	0.9	3	12074.9239	1.1	3	11940.2620	1.6	2	11747.9011		1
5	3	2	11762.1629	2.1	2	12076.8835	0.8	2	11941.9341		1	11749.1110		1
5	4	2	11825.0735	0.9	2	12135.2175	1.0	3	12004.0314		1	11816.5182		1
5	4	1	11825.1343	0.8	2	12135.2920	1.0	2	12004.1929	3.3	2	11816.4963		1
5	5	1	11907.0201		1	12210.8585	8.7	2	12085.0067	2.2	3	11891.2239		1
5	5	0	11907.0196		1	12210.8610	5.6	2	12085.0072	8.3	2	11891.2182		1
6	0	6	11721.2073		1	12038.4142	2.3	2	11900.3132		1			
6	1	6	11721.5283	0.0	2	12038.7057	1.0	2	11900.8420		1			
6	1	5	11771.1746	0.6	2	12087.9042	1.1	2	11949.2074	1.0	2	11753.5254		1
6	2	5	11777.0988	1.4	3	12094.4356 B	0.4	3	11957.2585		1	11760.8682		1
6	2	4	11797.7721	2.2	2	12118.2606	0.7	2	11979.9185	0.1	2	11784.3861		1
6	3	4	11830.9469	0.9	3	12146.8076	0.8	2	12011.2237	2.0	2	11819.3939		1
6	3	3	11836.4175	3.6	2	12152.0390	1.7	2	12015.7957		1	11822.8269	3.0	2
6	4	3	11895.9639	0.3	3	12207.9014	4.7	2	12075.3080		1	11889.1997		1
6	4	2	11896.2535	0.3	2	12208.2424		1	12075.8832		1	11888.9613		1
6	5	2	11977.6746	2.9	3	12284.1760	0.5	2				11963.1010		1
6	5	1	11977.7551		1	12284.2654	1.7	2	12155.9672		1	11963.1334		1
6	6	1	12077.0529		1	12374.4762		1	12253.1220		1	12063.4603		1
6	6	0	12077.0528		1	12374.4761		1	12253.1277		1	12063.4598		1
7	0	7	11790.1153	3.2	2	12107.9238		1	11969.2691		1			
7	1	7	11790.2367	4.6	3	12107.7038		1	11969.4466		1			
7	1	6	11851.5181	2.9	2	12169.3986	2.4	3	12029.9920		1	11834.4572		1
7	2	6	11854.6350	2.5	2	12172.4191	1.7	2	12034.8717	0.0	2	11838.7082		1
7	2	5	11887.2847	3.3	2	12207.7086	1.0	3	12068.7341	6.2	2			
7	3	5	11912.8246	0.4	3	12230.1524	0.4	2	12093.4190		1	11902.9765		1
7	3	4	11923.2861	3.4	3	12241.1745	2.6	3						
7	4	4	11978.9394	0.4	2	12292.7800	1.7	3	12158.4671	2.2	3	11974.1578 T		1
7	4	3	11979.9768	1.0	2	12294.1652	2.3	3						
7	5	3	12060.3995	1.4	2	12369.6263	2.8	3	12238.9989	0.8	2	12046.7738		1

Note: "B" and "T" denotes an energy level derived from a blended line and with tentative assignment, respectively. Energy levels marked by "*" were labelled on the basis of the effective Hamiltonian calculations (see text) N is the number of lines used for the upper energy level determination and σ denotes the corresponding experimental uncertainty in $10^{-3}\,cm^{-1}$ units.

Table 2 (*continued*)

J	K_a	K_c	(311)			(113)			(212)			(410)		
			E_{obs}	σ	N	E_{obs}	σ	N	E_{obs}	σ	N	E_{obs}	σ	N
7	5	2	12060.5308	1.2	2	12369.8452	3.5	3	12238.8805		1	12046.8826		1
7	6	2	12159.6848	1.9	2	12463.8274	0.3	2	12335.4375		1	12146.4367		1
7	6	1	12159.6847	2.1	2	12463.8296	1.7	2						
7	7	1	12276.8432		1	12564.9998		1	12446.3999		1	12264.9685		1
7	7	0	12276.8433		1	12564.9999		1	12446.4003		1	12264.9684		1
8	0	8	11868.0142		1	12183.0877	0.7	2	12047.0019		1	11851.0584		1
8	1	8	11868.0529		1	12186.1573	0.5	2	12047.2756		1			
8	1	7	11940.6559		1	12261.1922	1.0	2				11924.0794		1
8	2	7	11942.0601	0.7	3	12260.1709	1.0	2	12122.2295		1	11926.1989 T		1
8	2	6	11985.6323		1	12307.8473	1.3	2	12168.4737	3.0	2	11973.3391		1
8	3	6	12005.7984	1.6	3	12324.5409	1.5	3	12190.1190	2.9	2	11997.8308		1
8	3	5	12024.1785		1	12344.0652	1.1	2	12204.8487		1			
8	4	5	12073.7925	2.6	3	12389.6819	2.6	2	12252.2417	1.2	2	12070.9572		1
8	4	4	12076.6036 B		1	12393.0713	1.3	3	12257.7091	4.7	2	12072.0153		1
8	5	4	12155.1437	2.0	2	12467.1389	2.1	2	12334.2542		1			
8	5	3	12155.4182	2.5	2	12467.6593	4.4	2	12333.8373	3.7	2	12142.6555		1
8	6	3	12254.2769	1.7	2	12563.3342 B		1	12429.8051		1			
8	6	2	12254.2750	0.6	2	12563.3300 B		1				12241.3985		1
8	7	2	12371.5648	2.0	2	12656.3741		1	12539.2583		1	12360.9128		1
8	7	1	12371.5646	2.0	2	12656.3738		1	12539.2625		1	12360.9124		1
8	8	1	12508.9424		1	12781.8823		1	12681.7237 T		1			
8	8	0	12508.9425		1	12781.8824		1	12681.7238 T		1			
9	0	9	11954.9304		1	12271.9775	1.8	2						
9	1	9	11954.9637		1	12271.0933	1.1	2	12134.2799		1	11937.8795		1
9	1	8	12038.4507	1.3	2	12353.5122		1	12217.4635 T	8.9	2			
9	2	8	12039.0818		1	12357.5503	1.8	2	12219.1171		1	12023.1070	0.5	2
9	2	7	12104.2313		1	12417.2897		1						
9	3	7	12109.5271		1	12429.9036		1	12292.8951		1	12093.6979		1
9	3	6	12138.1573	1.2	2	12459.8932	3.3	2	12319.1972		1			
9	4	6	12180.4033	1.9	2	12498.3144		1				12179.7447		1
9	4	5	12186.8401	0.4	2	12505.7420	0.5	2						
9	5	5	12261.9443	1.7	2	12576.6149		1						
9	5	4	12262.6869		1	12577.8317		1						
9	6	4	12360.7621		1							12347.1950		1
9	6	3	12360.7663		1							12348.3055		1
9	7	3	12478.2786	2.4	2	12760.5118		1	12644.7384	0.2	2	12468.9756		1
9	7	2	12478.2785	2.8	2	12760.5114		1	12644.9690		1			
9	8	2	12616.0932 B		1	12886.8453		1				12606.7623		1
9	8	1	12616.0928 B		1	12886.8449		1				12606.7620		1
10	0	10	12050.9296		1	12368.1736		1	12230.8571	0.1	2	12033.5048	0.1	2
10	1	10	12049.9898		1	12368.8767	2.8	2	12231.0752	4.8	2			
10	1	9	12145.0506		1				12324.3609	2.1	2			
10	2	9	12145.8158		1	12465.2300	2.1	2	12325.4981		1			
10	2	8	12220.5564		1				12399.1677		1			
10	3	8	12223.1435		1							12211.2299		1
10	3	7	12264.0660	1.2	2	12587.4923		1	12444.7092	1.0	2			
10	4	7	12298.4158	1.7	2							12283.7673		1
10	4	6	12310.9808		1									
10	5	6	12380.7609	0.4	2	12697.7712 T		1						
10	5	5	12382.5877	0.8	2							12370.7229		1
10	6	5	12479.6345		1									
10	6	4	12479.6541 B		1							12467.3707		1
10	7	4	12596.9981	0.9	2									
10	7	3	12596.9971	0.3	2				12762.1229 T		1			
11	0	11	12155.6220		1	12473.7279	0.5	2	12335.1844		1	12138.3176		1
11	1	11	12155.6462		1	12473.7516		1	12334.6663	5.0	2	12139.1455		1
11	1	10	12260.6023		1	12576.4437		1						
11	2	10	12260.1075		1	12573.6000		1	12441.6251		1			
11	2	9	12348.3510		1									
11	3	9	12349.2518		1									
11	3	8	12400.4080		1	12725.3106		1						
11	4	8	12427.1340 B		1							12414.0973 *		1

(*continued on next page*)

Table 2 (*continued*)

J	K_a	K_c	(311)			(113)			(212)			(410)		
			E_{obs}	σ	N	E_{obs}	σ	N	E_{obs}	σ	N	E_{obs}	σ	N
11	4	7	12448.8985	2.8	2									
11	5	7	12511.3096		1									
11	5	6	12515.5346	5.1	3									
11	6	6	12610.5525 B		1									
11	6	5	12610.8727		1									
11	7	5	12727.7454		1									
11	7	4	12727.7491	1.4	2									
12	0	12	12269.5295		1	12588.1336 B		1	12447.0856		1			
12	1	12	12269.7299 B		1	12588.1443 B		1	12447.2335		1			
12	1	11	12384.1237		1	12700.6689		1				12368.2327		1
12	2	11	12384.6002		1	12700.6756		1						
12	2	10	12483.2159		1									
12	3	10	12483.3490		1									
12	3	9	12553.9809		1									
12	4	9	12570.8678		1									
12	4	8	12599.8631		1									
12	5	8	12652.8021		1									
12	5	7	12662.0061 T		1									
12	6	7	12753.7561		1									
13	0	13	12392.4712		1	12711.5127		1	12570.5854		1	12374.5926 BT		1
13	1	13	12392.4759		1	12711.5174		1	12570.5848		1	12374.5880 BT		1
13	1	12	12517.8529		1									
13	2	12	12518.0470		1									
13	2	11	12627.7993		1									
13	3	11	12627.1420		1									
13	3	10	12716.6937		1									
13	4	10										12700.4488 T		1
14	0	14	12524.3420		1	12843.8898		1						
14	1	14	12524.3444		1	12843.8012		1						
14	1	13	12660.0919		1									
14	2	13	12660.1062		1									
14	3	12	12780.3592		1									
14	3	11	12880.0739 B		1									
14	4	11	12881.8974		1									
15	0	15	12665.1172		1									
15	1	15	12665.1178		1									
15	1	14	12811.4079		1									
15	2	13	12942.6895		1									
16	0	16	12814.8316		1									
16	1	16	12814.8318		1									

first stage of this study, as well as new data from Refs. [3,16,17] were combined and used by Shirin et al. [18] for a further optimization of the D_2O PES. A new synthetic spectrum [18], referred below as "calculation 2", was generated with the new D_2O PES and again with the DMS of Ref. [13]. This was successfully applied to complete the assignment of the weak D_2O lines in the 11400–11900 cm^{-1} spectral region. The good agreement between these new calculations and the observed spectra is illustrated in Figs. 2 and 3. In total, 530 precise new experimental energy levels were derived for the eight vibrational states as summarized in Table 1. Note that 47 of the energy levels for the (311) vibrational state were also determined from the analysis of the FTS spectrum [4].

The whole set of energy levels are given in Tables 2 and 3. We estimate the accuracy of the observed energy levels as 0.002 cm^{-1} on average for levels confirmed by the combination differences. Energy levels derived from blended lines are determined with less accuracy and are specially marked. A line list counting 956 D_2O transitions that corresponds to 840 lines is attached to this paper as Supplementary Material. In the case of multiple assignments to the same observed line, we followed HITRAN [19] by distributing the experimental intensity among the different components in proportion to their calculated values.

Deviations of the observed energy levels from "calculation 1" and "calculation 2" are shown in Fig. 4 for the $[J0J]$ energy levels (using the notation $[JK_aK_c]$) of the strongest assigned bands. "Calculation 2" is much more precise, with maximum (obs. − calc.) deviation not exceeding 0.13 cm^{-1}. The pronounced deviation of the (113) [10010] level at 12368.1736 cm^{-1} from the smooth behaviour of the (obs. − calc.) curve for the (113) vibrational state ("calculation 2") is caused by a strong resonance interaction with the (410) [1056] level at 12369.25 cm^{-1}. The origin of the (033)–(000) band at 11605.79 cm^{-1}

Table 3
Rovibrational term values (cm^{-1}) of the (033), (132), (231), and (330) vibrational states of D_2O

J	K_a	K_c	E_{obs}	σ	N
(033)					
1	0	1	11617.7389		1
2	0	2	11641.0773		1
2	1	2	11648.6253	3.6	2
2	2	1	11686.6080		1
2	2	0	11687.1483		1
3	0	3	11674.8083	2.3	2
3	1	3	11679.8151		1
3	1	2	11696.9674		1
3	2	1	11725.0507	3.6	2
3	3	1	11778.1034		1
3	3	0	11778.1630		1
4	1	4	11720.9049		1
4	1	3	11749.0694		1
4	2	2	11776.8804	4.7	2
4	3	2	11826.9343	1.1	2
4	4	1	11901.9665		1
4	4	0	11901.9608		1
5	0	5	11770.0423		1
5	1	5	11771.5751	0.3	2
5	1	4	11812.6647	1.0	2
5	2	3	11842.8061		1
5	3	2	11889.1556	3.1	2
5	4	1	11963.3786	2.9	2
5	5	1	12056.9534		1
5	5	0	12056.9529		1
6	0	6	11830.9575		1
6	1	6	11831.6619	0.7	2
6	1	5	11886.3966	1.5	2
6	2	5	11897.4773	0.1	2
6	2	4	11922.0840		1
6	3	4	11961.1655	2.0	2
6	4	3	12037.1626		1
6	4	2	12037.4182		1
7	0	7	11900.5462	5.0	3
7	1	6	11969.5779	0.9	2
7	2	5	12014.1108		1
7	4	3	12124.2703	1.3	2
8	2	7	12066.2172		1
8	8	1	12692.1246 T		1
8	8	0	12692.1247 T		1
9	0	9	12066.1126		1
9	1	8	12165.5340 *		1
9	2	7	12231.5359		1
10	3	8	12366.7414		1
11	0	11	12268.3747		1
(132)					
3	3	1	11618.4223		1
4	2	2	11613.0982		1
4	3	2	11666.6726		1
4	3	1	11667.0128		1
4	4	1	11743.7133		1
4	4	0	11743.7225		1
5	3	3	11726.9456	3.9	2
5	4	2	11803.7760		1
5	4	1	11803.8378 B		1
6	3	4	11799.9561 *		1
6	3	3	11801.9944		1
6	4	3	11875.8443		1
6	4	2	11876.1132		1
7	3	5	11881.6272		1
7	4	4	11959.8077		1
7	4	3	11960.6105		1
8	4	5	12055.4020		1
8	4	4	12058.0769		1
(231)					
5	4	1	11660.7418	0.8	2
5	5	0	11764.2365		1
6	5	2	11835.6840		1
6	5	1	11834.8121 *	0.5	2
7	5	2	11918.6772	4.9	2
8	5	4	12015.1156		1
9	6	3	12241.8549		1
10	3	8	12052.2767		1
10	4	7	12140.6333 BT		1
(330)					
8	5	4	11988.0334		1
9	5	5	12096.9431		1
9	7	3	12361.0071 *		1
9	7	2	12361.0268 *		1
11	5	7	12351.3114		1

Note: "B" and "T" denotes an energy level derived from a blended line and with tentative assignment, respectively. Energy levels marked by "*" were labelled on the basis of the effective Hamiltonian calculations (see text) N is the number of lines used for the upper energy level determination and σ denotes the corresponding experimental uncertainty in 10^{-3} cm^{-1} units.

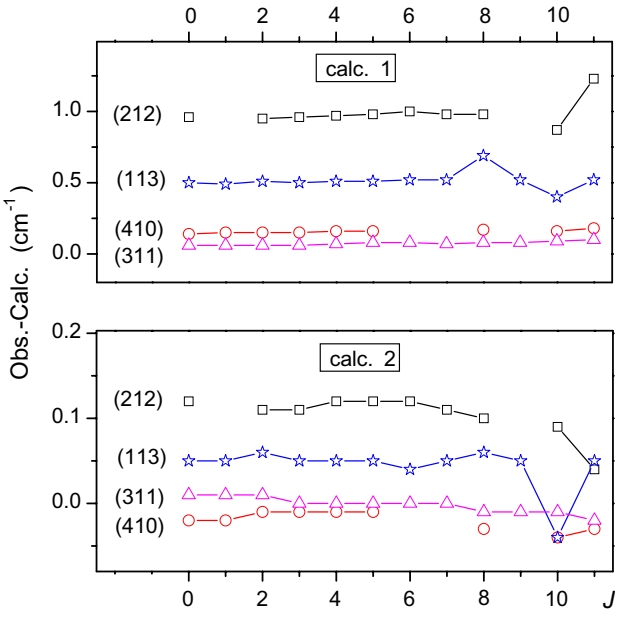

Fig. 4. Variation of the difference between the experimental and calculated energy levels versus J, for the $K_a = 0$ energy sublevels of the four of the analyzed vibrational states corresponding to the stronger bands. Upper and lower panels illustrate the results of the variational calculations of Ref. [14] (calc. 1) and Ref. [18] (calc. 2) respectively. Note the different scales adopted for the ordinate axis.

(see Table 1) could be derived with estimated accuracy not worse than $\pm 0.05\ cm^{-1}$, from the (obs. – calc.) trend for the $[J0J]$ energy levels.

The relative experimental line intensities were retrieved for every 12 cm^{-1} wide spectral window, and then scaled against the "calculation 2" values. The FTS intensities [4] could not be used for this purpose as only 71 lines were observed in the whole region, leaving large spectral sections without any data. The quality of "calculation 2" intensities based on Schwenke and Partridge DMS [13] was checked in Ref. [4] by the comparison with 1175 precise experimental intensities in the 10 000–13 160 cm^{-1} spectral region and found to be very high with an average I_{obs}/I_{calc} intensity ratio of 1.09. Integrated observed and calculated intensities are given in Table 1 for all the bands considered. Fig. 5 displays the observed to calculated intensity ratio versus the calculated line intensity for the whole spectral region under study.

For the spectral assignments, we adopted, mostly, the rovibrational labelling provided by Ref. [15], which followed the labelling procedure adopted by Partridge and Schwenke in their original work [11]. This procedure is based on inspecting the contributions of the basis functions into the resulting wave function of the analyzed energy level. However, as high rovibrational excitation leads to a considerable mixing of the wave functions, this procedure may lead to ambiguities in the ascribing the vibrational and rotational quantum numbers.

Indeed, we faced a problem with ambiguous labelling for a number of levels. Thus, in Ref. [15] the (4 1 0) state is associated with two sets of the energy levels, separated by about 200 cm^{-1}. The higher set can correctly be attributed to the (2 1 2) state. However, it proved difficult to relabel the seven energy levels which are marked in Tables 2 and 3 by an asterisk. Calculations within an effective Hamiltonian (EH) were performed to confirm new labels. As a result, five of the seven noted energy levels could be relabelled with confidence. However, the labelling proposed here for the [9 7 3] and [9 7 2] levels of the (3 3 0) state at 12 361.0071 and 12 361.0268 cm^{-1}, respectively must be considered with caution.

Despite employing very accurate calculations, we consider some of our assignments (marked by "T' in the line list and in Tables 2 and 3) as tentative. These cases are single identifications (i.e. not confirmed by CD) associated with either a very weak line, or as a second or third component of an already assigned line. Fig. 6 shows the D_2O experimental stick spectrum along with weak unobserved predicted lines. The intensities of the unobserved lines are mostly, not larger than 10^{-27} cm/molecule which is the detection limit of the present recording. The stronger unobserved lines above 11 800 cm^{-1} are probably obscured by stronger D_2O or HDO lines.

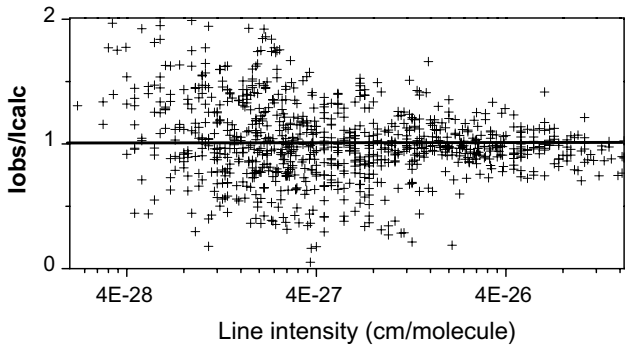

Fig. 5. Variation of the ratio of the ICLAS line intensities to those predicted by the new variational calculations of Ref. [18], versus the calculated intensity values.

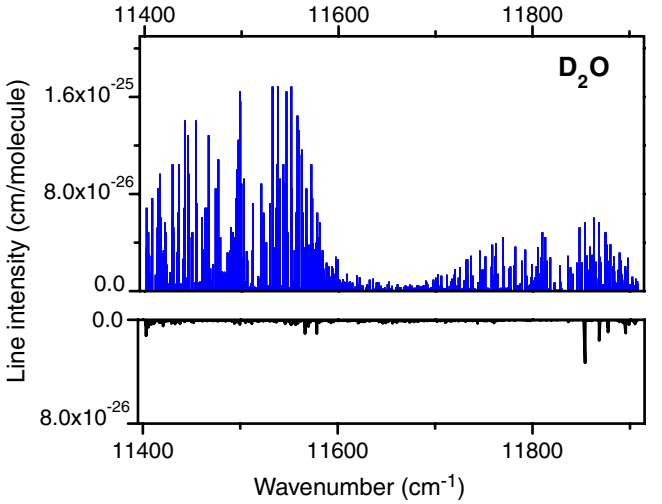

Fig. 6. Upper panel: ICLAS stick spectrum between 11 400 and 11 900 cm^{-1}. Lower panel: transitions predicted by the variational calculations of Ref. [18] remaining unobserved.

4. Conclusion

The performance of the ICLAS technique combined with the use of a highly enriched sample containing 98% of deuterium yielded a detailed D_2O absorption spectrum for the 11 400–11 900 cm^{-1} spectral range, including regions where the HDO or H_2O transitions are much stronger than those of D_2O for pure species. The small number of HDO lines and the absence of H_2O transitions in our ICLAS spectra was of valuable advantage in the spectral analysis. A list of 840 lines was constructed enlarging considerably the set of 71 lines observed by Fourier Transform spectroscopy in the same region [4].

A new variational calculation of the D_2O line positions and intensities [18] based on an optimised PES and Schwenke and Partridge DMS [13] was used for the spectrum identification and proved to be very accurate (within 0.13 cm^{-1}) for the line positions. The complete assignment of the observed spectrum yielded 530 new rovibrational energy levels belonging to eight vibrational states. The observed D_2O lines in the 11 400–11 900 cm^{-1} spectral region comprises 90% of the predicted total D_2O absorption due to lines stronger than 8.0×10^{-29} cm/molecule.

Due to the change in atomic masses of D_2O compared to H_2O, the D_2O variational calculations are sensitive to adiabatic and nonadiabatic corrections to the H_2O PES obtained in the Born–Oppenheimer approximation. Thus, the results obtained in this study both extend our knowl-

edge about the energy levels structure of the D_2O molecule and may be of importance for further improvement of the mass dependent PES of the H_2O molecule.

Acknowledgments

This work, performed in the framework of the European research network QUASAAR (MRTN-CT-2004-512202), is jointly supported by the INTAS foundation (project 03-51-3394) as well as a collaborative project between CNRS and RFBR (PICS Grant No. 05-05-22001) and the Russian Foundation for Basic Research. It is part of an effort by the Task Group of the International Union of Pure and Applied Chemistry (IUPAC, Project No. 2004-035-1-100) to compile, determine, and validate, both experimentally and theoretically, accurate frequency, energy level, line intensity, line width, and pressure effect spectral parameters of all major isotopologues of water. AC (Grenoble) is grateful for the financial support provided by Programme National LEFE of CNRS (INSU). OML and OVN (Tomsk) acknowledge the financial support from UCL and the Royal Society for visits to UCL. We thank Alain Jenouvier (GSMA, Reims) for communicating us the D_2O line list attached to Ref. [4], prior to publication.

Appendix A. Supplementary data

Supplementary data for this article are available on ScienceDirect (www.sciencedirect.com) and as part of the Ohio State University Molecular Spectroscopy Archives (http://msa.lib.ohio-state.edu/jmsa_hp.htm).

References

[1] O.N. Ulenikov, S.M. Hu, E.S. Bekhtereva, G.A. Onopenko, S.-G. He, X.-H. Wang, J.-J. Zheng, Q.-S. Zhu, J. Mol. Spectrosc. 210 (2001) 18–27.

[2] S.-M. Hu, O.N. Ulenikov, E.S. Bekhtereva, G.A. Onopenko, S.-G. He, H. Lin, J.-X. Cheng, Q.-S. Zhu, J. Mol. Spectrosc. 212 (2002) 89–95.

[3] O.V. Naumenko, O. Leshchishina, S. Shirin, A. Jenouvrier, S. Fally, A.C. Vandaele, E. Bertseva, A. Campargue, J. Mol. Spectrosc. 238 (2006) 79–90.

[4] A. Jenouvrier, S. Fally, A.C. Vandaele, O.V. Naumenko, O. Leshchishina, S. Shirin, J. Tennyson, J. Mol. Spectrosc., to be submitted for publication.

[5] O. Naumenko, O. Leshchishina, A. Campargue, J. Mol. Spectrosc. 236 (2006) 58–69.

[6] A. Charvat, A.A. Kachanov, A. Campargue, D. Permogorov, F. Stoeckel, Chem. Phys. Lett. 14 (1993) 495–501.

[7] A. Kachanov, A. Charvat, F. Stoeckel, J. Opt. Soc. Am. B 11 (1994) 2412–2419.

[8] A. Garnache, A. Liu, L. Cerutti, A. Campargue, Chem. Phys. Lett. 416 (2005) 22–27.

[9] S. Hu, A. Campargue, Z.-Y. Wu, Y. Ding, A.-W. Liu, Q.-S. Zhu, Chem. Phys. Lett. 372 (2003) 659–667.

[10] M. Bach, S. Fally, P.-F. Coheur, M. Carleer, A. Jenouvrier, A.C. Vandaele, J. Mol. Spectrosc. 232 (2005) 341–350.

[11] H. Partridge, D.W. Schwenke, J. Chem. Phys. 106 (1997) 4618–4639.

[12] O.L. Polyansky, N.F. Zobov, S. Viti, J. Tennyson, P.F. Bernath, L. Wallace, Science 277 (1997) 346–349.

[13] D.W. Schwenke, H. Partridge, J. Chem. Phys. 113 (2000) 6592–6597.

[14] S.V. Shirin, N.F. Zobov, O.L. Polyansky, J. Tennyson, T. Parekunnel, P.F. Bernath, J. Chem. Phys. 120 (2004) 206–210.

[15] S.A. Tashkun, private communication.

[16] N.F. Zobov, R.I. Ovsannikov, S.V. Shirin, O.L. Polyansky, J. Tennyson, A. Janka, P.F. Bernath, J. Mol. Spectrosc. 240 (2006) 112–119.

[17] S.N. Mikhailenko, G.C. Mellau, E.N. Starikova, S.A. Tashkun, Vl.G. Tyuterev, J. Mol. Spectrosc. 233 (2005) 32–59.

[18] S.V. Shirin, N.F. Zobov, O.L. Polyansky, J. Mol. Spectrosc., submitted for publication.

[19] L.S. Rothman, D. Jacquemart, A. Barbe, D. Chris Benner, M. Birk, L.R. Brown, M.R. Carleer, C. Chackerian Jr., K. Chance, V. Dana, V.M. Devi, J.-M. Flaud, R.R. Gamache, A. Goldman, J.-M. Hartmann, K.W. Jucks, A.G. Maki, J.Y. Mandin, S.T. Massie, J. Orphal, A. Perrin, C.P. Rinsland, M.A.H. Smith, J. Tennyson, R.N. Tolchenov, R.A. Toth, J. Vander Auwera, P. Varanasi, G. Wagner, J. Quant. Spectrosc. Radiat. Transfer 96 (2005) 139–204.